Applied Physics Letters

RESEARCH ARTICLE | AUGUST 05 2024

Origin of exponentially large increase in the leakage current in alumina films depending on the ALD synthesis temperature

A. A. Gismatulin ; Yu. N. Novikov ; N. V. Andreeva ; D. S. Mazing ; V. A. Gritsenko

Appl. Phys. Lett. 125, 062901 (2024)
https://doi.org/10.1063/5.0217150

Applied Physics Letters ARTICLE pubs.aip.org/aip/apl

Origin of exponentially large increase in the leakage current in alumina films depending on the ALD synthesis temperature

Cite as: Appl. Phys. Lett. **125**, 062901 (2024); doi: 10.1063/5.0217150
Submitted: 3 May 2024 · Accepted: 21 July 2024 ·
Published Online: 5 August 2024

A. A. Gismatulin,[1,a)] Yu. N. Novikov,[1] N. V. Andreeva,[2] D. S. Mazing,[2] and V. A. Gritsenko[1,3]

AFFILIATIONS

[1]Rzhanov Institute of Semiconductor Physics SB RAS, 13 Lavrentiev aven., 630090 Novosibirsk, Russia
[2]St. Petersburg State Electrotechnical University LETI, 5 Popov str., 197022 St. Petersburg, Russia
[3]Novosibirsk State Technical University, 20 Marx aven., 630073 Novosibirsk, Russia

[a)]Author to whom correspondence should be addressed: aagismatulin@isp.nsc.ru

ABSTRACT

Amorphous aluminum oxide a-Al_2O_3 deposited by atomic layer deposition (ALD) is widely used in nonvolatile memory devices. In this paper, the leakage current dependence on the ALD synthesis temperature is investigated by six charge transport models: Schottky effect, thermally assisted tunneling at a contact, Frenkel effect, Hill-Adachi model of overlapping Coulomb potentials, Makram-Ebeid and Lannoo multiphonon isolated trap ionization model, and Nasyrov–Gritsenko model of phonon-assisted tunneling between neighboring traps. It is shown that the leakage current exponentially increases with the ALD synthesis temperature, which is related to the increase in trap concentration.

Amorphous aluminum oxide (a-Al_2O_3) is used in modern TANOS (TaN/Al_2O_3/Si_3N_4/SiO_2/Si) NAND flash memory devices based on the localization effect of electrons and holes at traps in silicon nitride.[1,2] Currently, a-Al_2O_3 is intensively studied as an active layer in the memristor memory.[3–10] When a short (for example, in this paper,[11] the pulse duration of 100 ps was reached) voltage pulse is applied, the memristor switches from a high-resistance state (HRS) to a low-resistance state (LRS). To switch back from a LRS to a HRS, voltage pulse of a different polarity or a different value is used. At the same time, HRS and LRS are retained, when the voltage is off, for 10 years at 85 °C. Typically, the memory window [the HRS (R_{OFF}) to the LRS (R_{ON}) ratio] in a memristor based on different materials is in the range of 2–4 orders of magnitude.[12–14] a-Al_2O_3 is a unique material in which the R_{OFF}/R_{ON} ratio can reach six orders of magnitude.[15]

In microelectronic devices, a-Al_2O_3 films are grown by the atomic layer deposition (ALD) method. The dependence of ALD a-Al_2O_3 film properties on the synthesis temperature has already been noted,[16,17] but no correlation has been made yet with leakage currents. One of the most important ALD a-Al_2O_3 parameters is the leakage current, which determines the breakdown voltage. The charge transport in stoichiometric a-Al_2O_3 films, at low trap concentrations, is limited by the multiphonon isolated trap ionization model.[18,19]

The leakage current value strongly depends on the a-Al_2O_3 synthesis conditions in the ALD process. Increasing the synthesis temperature of ALD a-Al_2O_3 leads to an exponential increase in the a-Al_2O_3 leakage current.[20] In the experiment, a wide range of leakage currents in silicon nitride[21] and silicon oxide[22] films is observed. Currently, there is no universal explanation for the wide range nature of leakage currents in dielectric films. The aim of this work is to establish the physical cause of the wide range of alumina leakage currents at different ALD synthesis temperatures.

Before the ALD process, the substrate surface was treated as follows: the removal of organic contaminants from the substrate surface in a solution of H_2O:NH_4OH:H_2O_2 heated to 75 °C for 10 min; rinsing the substrate in de-ionized water; removal of native oxide from the substrate surface in a 10% HF solution at room temperature for 2 min; and rinsing again the substrate in de-ionized water and drying the substrate with compressed air.

The synthesis of the functional a-Al_2O_3 layer was carried out by the ALD method using trimethylaluminum (TMA) and de-ionized water as precursors. The a-Al_2O_3 structures were synthesized at 160, 200, and 250 °C to reveal the difference in the charge transport mechanism in the a-Al_2O_3 layer at different ALD synthesis temperatures. The thickness of the deposited ALD a-Al_2O_3 layers was controlled by

ellipsometry and amounted to $d = 37 \pm 1$ nm. A magnesium (Mg) metal contact was selected due to the work function to exclude the hole conductivity in the structure. In the Mg contact case, unipolar electronic conductivity occurred in the n-Si/Al_2O_3/Mg structure. The Mg contact area was 0.5 mm^2. The current–voltage characteristics were carried out on a Keithley 2400 electrometer. The temperature range of 300–375 K was set in the Linkam LTS420E cell and temperature controller Linkam T95.

The measurements of the current–voltage characteristics were carried out on n-Si/Al_2O_3/Mg structures at different temperatures. The experimental data of current–voltage characteristics were recalculated in the current density dependence on the electric field [*lg(j)-F*] characteristics taking into account the known sample thickness and contact area. We assume that the leakage current increases with the increasing ALD synthesis temperature, and the charge transport mechanism is then different.

The Schottky effect is a phenomenon where the interface barrier height decreases at strong applied electric field [Fig. 1(a)]. The Schottky effect current density is described by the following equation:[23]

$$j = AT^2 \exp\left(-\frac{W_0 - \left(\frac{e^3}{4\pi\varepsilon_\infty\varepsilon_0}\right)^{1/2}\sqrt{F}}{kT}\right), \quad (1)$$

$$A = \frac{4\pi m^* k^2 e}{m_e h^3} = 120.4\frac{m^*}{m_e}\left[\frac{A}{cm^2K^2}\right], \quad (2)$$

where j—current density, A—Richardson-Dushman constant, T—temperature, W_0—potential barrier height at the n-Si/Al_2O_3 interface, F—electric field, k—Boltzmann constant, e—electron charge, $\varepsilon_\infty = n^2$—high frequency dielectric permittivity, n—refractive index, ε_0—dielectric constant, m^*—electron effective mass, m_e—electron mass, and h—Plank constant.

The *lg(j)-F* characteristics of the n-Si/Al_2O_3/Mg structure synthesized at 250 °C were measured in the silicon substrate accumulation mode at a positive potential on Mg. The charge transport simulation by the Schottky effect is shown in Fig. 1(a). The Schottky effect formally describes the experimental data of the n-Si/Al_2O_3/Mg structure synthesized at 250 °C, but the fitting parameters obtained during simulation do not correspond to the given structure and Al_2O_3 material. The potential barrier height, at the n-Si/Al_2O_3 interface, value $W_0 = 1.25$ eV was determined from current density temperature dependence. However, the theoretical potential barrier height at the Si/Al_2O_3 interface value W_0 is around 2.1 eV.[24] The high-frequency dielectric constant obtained by Schottky effect simulation is anomalously small ($\varepsilon_\infty = 0.85$), compared to the experimental ellipsometric data ($\varepsilon_\infty = n^2 = 1.6^2 = 2.56$). In addition, the Schottky effect simulation effective mass value ($m^* = 3 \times 10^{-8}\, m_e$) is also anomalously small. All of those fitting parameters indicate that the Schottky effect cannot describe the charge transport in the n-Si/Al_2O_3/Mg structure synthesized at 250 °C.

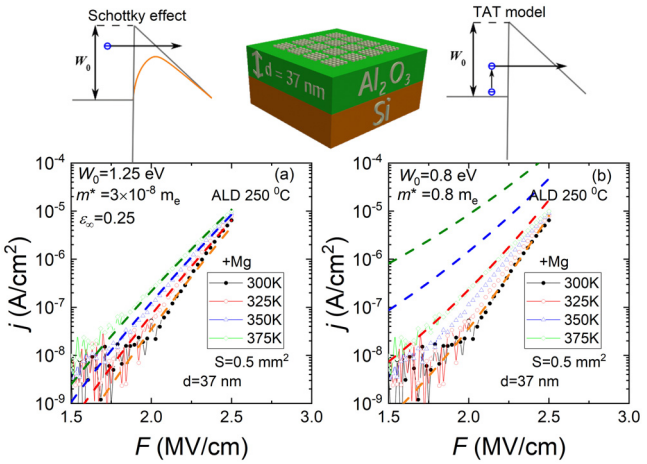

FIG. 1. Current density dependence on the electric field in n-Si/Al_2O_3/Mg (ALD 250 °C) at different temperatures and the theoretical dependences obtained based on (a) the Schottky effect and (b) the thermally assisted tunneling (TAT) at a contact. Above are a schematic representation of the Schottky effect, the TAT at a contact model, and a 3D image of the n-Si/Al_2O_3/Mg structure.

The thermally assisted tunneling (TAT) at a contact is described in the case when electrons are tunneling through the triangle barrier at a higher energy than the Fermi level in the metal [Fig. 1(b)]. The current density expression for the TAT at a contact has the following form:[25,26]

$$j = CF\exp\left(-\frac{W_0 - \frac{1}{6}\left(\frac{heF}{4\pi kT\sqrt{m^*}}\right)^2}{kT}\right), \quad (3)$$

where $C = \sqrt{2\pi m^* kT}\left(\frac{e}{h}\right)^2$.

The TAT at a contact model only has two fitting parameters, and simulation by the TAT at a contact model gives the effective mass value of $m^* = 0.8m_e$ and potential barrier height, at the n-Si/Al_2O_3 interface, value of $W_0 = 1.27$ eV. The simulated potential barrier height value is still lower than the theoretical one. The TAT simulation with those parameters can only describe the experimental data at 300 K and cannot describe the experimental current density data at other temperatures [Fig. 1(b)]. Therefore, the TAT at a contact model cannot describe the charge transport in the n-Si/Al_2O_3/Mg structure synthesized at 250 °C.

A current density in the dielectric bulk is determined by following expression:[27]

$$j = eNPl \approx eN^{2/3}P, \quad (4)$$

where N—filled trap concentration, P—trap ionization probability, and l—electron mean free path to the next capture on the trap, which is approximately equal to a—average distance between traps ($l \approx a = N^{-1/3}$).

The Frenkel mechanism is the thermal ionization of an isolated Coulomb trap in a strong electric field.[28,29] The trap ionization probability of isolated Coulomb traps by the Frenkel mechanism was given by the following expression:[28,29]

$$P = \nu\exp\left(-\frac{W - \sqrt{\frac{e^3}{\pi\varepsilon_\infty\varepsilon_0}F}}{kT}\right), \quad (5)$$

where W is the trap ionization energy and ν is the attempt-to-escape factor (electron collisions frequency with the walls of a potential well evaluated in the Frenkel model as W/h).

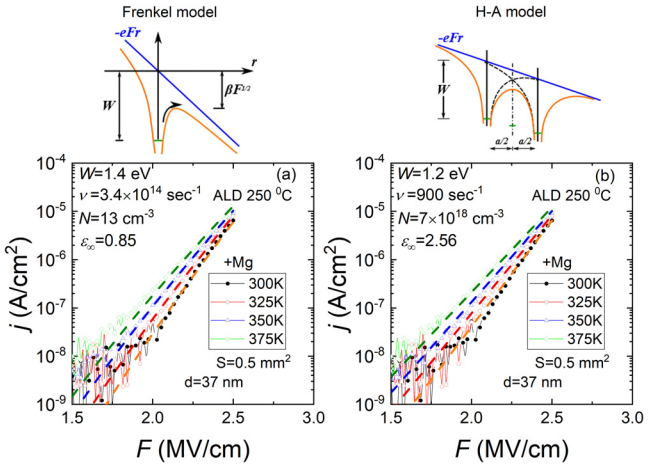

FIG. 2. Current density dependence on the electric field in n-Si/Al_2O_3/Mg (ALD 250 °C) at different temperatures and the theoretical dependences obtained based on (a) the Frenkel effect and (b) the Hill-Adachi (H-A) model of overlapping Coulomb potentials. Above is a schematic representation of the Frenkel model and the H-A model.

The charge transport simulation of the n-Si/Al_2O_3/Mg structure by the Frenkel effect is presented in Fig. 2(a). The trap ionization energy value was determined from the current density temperature dependence as $W = 1.4$ eV. From the known ionization energy value, the attempt-to-escape factor was found: $\nu = W/h = 3.4 \times 10^{14}\,\mathrm{s}^{-1}$. The remaining selected parameters are trap concentration and high-frequency dielectric constant. When simulating with the Frenkel effect, anomalously small values of trap concentration ($N = 13\,\mathrm{cm}^{-3}$) and high-frequency dielectric constant ($\varepsilon_\infty = 0.85$) are obtained. Therefore, the Frenkel effect does not describe the charge transport mechanism in the n-Si/Al_2O_3/Mg structure synthesized at 250 °C.

As the trap concentration increases, the distance between them becomes such that the ionization energy decreases due to the overlap of two neighboring Coulomb traps. The conductivity at a high Coulomb trap concentration is described by the Hill-Adachi (H-A) model of overlapping Coulomb potentials.[30,31] The ionization probability in the H-A model is given by the following expression:[30,31]

$$P = 2\nu \exp\left(-\frac{W - \dfrac{e^2}{\pi\varepsilon_\infty\varepsilon_0 a}}{kT}\right)\sinh\left(\frac{eFa}{2kT}\right). \tag{6}$$

The experimental data and simulation results obtained by using the H-A model are presented in Fig. 2(b). Model H-A qualitatively describes the charge transport in the n-Si/Al_2O_3/Mg structure with the trap concentration of $N = 7 \times 10^{18}\,\mathrm{cm}^{-3}$, high-frequency dielectric constant of $\varepsilon_\infty = 2.56$, and ionization trap energy of $W = 1.2$ eV. The attempt-to-escape factor used in model H-A is $\nu = W/h = 2.9 \times 10^{14}\,\mathrm{s}^{-1}$. However, from the experimental data, the H-A model predicts the abnormally low attempt-to-escape factor value of $\nu = 900\,\mathrm{s}^{-1}$. Therefore, the H-A model does not describe the charge transport mechanism in the n-Si/Al_2O_3/Mg structure synthesized at 250 °C.

Similar to the Frenkel effect, the multiphonon isolated trap ionization model of Makram-Ebeid and Lannoo (ME-L) describes the trap ionization in the case of a large distance between traps or a low trap concentration, but the ME-L model describes the multiphonon ionization of a neutral isolated trap instead of the Coulomb trap ionization in a strong electric field. In the ME-L model, the electron is excited into the conduction band due to the multiphonon absorption, where it moves along the electric field until it is captured by the neighboring trap. Such electron movements are repeated until the electron reaches the contact [Fig. 3(a)].[32] The multiphonon trap ionization probability of the ME-L model has the following form:[32]

$$P = \sum_n \exp\left(\frac{nW_{ph}}{2kT} - \frac{W_{opt} - W_t}{W_{ph}}\coth\frac{nW_{ph}}{2kT}\right) \times I_n\left(\frac{W_{opt} - W_t}{W_{ph}\sinh\left(W_{ph}/2kT\right)}\right)P_i. \tag{7}$$

Herein, $P_i = \frac{eF}{2\sqrt{2m^*(W_t + nW_{ph})}}\exp\left(-\frac{4}{3}\frac{\sqrt{2m^*}}{\hbar eF}(W_t + nW_{ph})^{3/2}\right)$, where W_t is the thermal trap energy, W_{opt} is the optical trap energy, W_{ph} is the phonon energy, I_n is the modified Bessel function, P_i is a tunneling probability through a triangular barrier, and $\hbar$ is the reduced Planck constant.

The experimental data and simulation results obtained by using the ME-L model are presented in Fig. 3(a). The comparison of the experimental data for the n-Si/Al_2O_3/Mg structure with the ME-L model is given with the parameters of thermal trap energy $W_t = 1.5$ eV and the optical trap energy of $W_{opt} = 3.0$ eV. However, the ME-L model predicts the low effective mass of $m^* = 0.05m_e$ and the unphysically low trap concentration value of $N = 0.6 \times 10^{14}\,\mathrm{cm}^{-3}$. With the obtained parameters, the ME-L model does not describe the charge transport in the n-Si/Al_2O_3/Mg structure synthesized at 250 °C.

At a high trap concentration, the distance between neutral traps is small. The Nasyrov–Gritsenko (N-G) model of phonon-assisted tunneling between neighboring traps takes into account the overlapping integral of neighboring neutral traps. After ionization, it is more

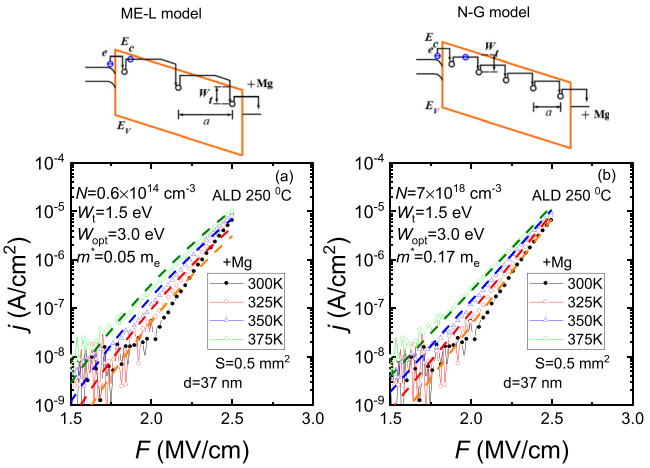

FIG. 3. Current density dependence on the electric field in n-Si/Al_2O_3/Mg (ALD 250 °C) at different temperatures and the theoretical dependences obtained based on (a) Makram-Ebeid and Lannoo (ME-L) model of multiphonon isolated trap ionization and (b) Nasyrov–Gritsenko (N-G) model of phonon-assisted tunneling between neighboring traps. Above is a schematic representation of the ME-L model and the H-A model.

TABLE I. Fitting parameters for all charge transport models for different samples. Red colored parameters are unfitted for simulating experimental data.

Sample	Schottky	TAT	Frenkel	H-A	ME-L	N-G
160 °C	$m^* = 4 \times 10^{-5}\, m_e$ $W_0 = 1.8$ eV $\varepsilon_\infty = 0.18$	$m^* = 1.0 m_e$ $W_0 = 1.36$ eV	$N = 8.0 \times 10^{14}$ cm^{-3} $W = 1.6$ eV $\nu = 3.8 \times 10^{14}$ s^{-1} $\varepsilon_\infty = 1$	$N = 5.0 \times 10^{18}$ cm^{-3} $W = 1.5$ eV $\nu = 7.8 \times 10^{4}$ s^{-1} $\varepsilon_\infty = 2.56$	$N = 4.0 \times 10^{18}$ cm^{-3} $m^* = 0.24 m_e$ $W_t = 1.5$ eV $W_{opt} = 3.0$ eV $W_{ph} = 60$ meV	$N = 5.0 \times 10^{18}$ cm^{-3} $m^* = 0.07 m_e$ $W_t = 2.2$ eV $W_{opt} = 4.4$ eV
200 °C	$m^* = 5 \times 10^{-9}\, m_e$ $W_0 = 1.25$ eV $\varepsilon_\infty = 0.25$	$m^* = 0.9 m_e$ $W_0 = 1.3$ eV	$N = 0.7$ cm^{-3} $W = 1.4$ eV $\nu = 3.4 \times 10^{14}$ s^{-1} $\varepsilon_\infty = 0.85$	$N = 6.0 \times 10^{18}$ cm^{-3} $W = 1.2$ eV $\nu = 67$ s^{-1} $\varepsilon_\infty = 2.56$	$N = 0.3 \times 10^{13}$ cm^{-3} $m^* = 0.05 m_e$ $W_t = 1.5$ eV $W_{opt} = 3.0$ eV $W_{ph} = 60$ meV	$N = 6.0 \times 10^{18}$ cm^{-3} $m^* = 0.19 m_e$ $W_t = 1.5$ eV $W_{opt} = 3.0$ eV
250 °C	$m^* = 3 \times 10^{-8}\, m_e$ $W_0 = 1.25$ eV $\varepsilon_\infty = 0.25$	$m^* = 0.8 m_e$ $W_0 = 1.27$ eV	$N = 13$ cm^{-3} $W = 1.4$ eV $\nu = 3.4 \times 10^{14}$ s^{-1} $\varepsilon_\infty = 0.85$	$N = 7.0 \times 10^{18}$ cm^{-3} $W = 1.2$ eV $\nu = 900$ s^{-1} $\varepsilon_\infty = 2.56$	$N = 0.6 \times 10^{14}$ cm^{-3} $m^* = 0.05 m_e$ $W_t = 1.5$ eV $W_{opt} = 3.0$ eV $W_{ph} = 60$ meV	$N = 7.0 \times 10^{18}$ cm^{-3} $m^* = 0.17 m_e$ $W_t = 1.5$ eV $W_{opt} = 3.0$ eV

advantageous for the electron to immediately tunnel to the neighboring trap, without entering the conduction band [Fig. 3(b)].[33] The trap ionization probability in the N-G model has the following form:[33]

$$P = \frac{2\sqrt{\pi\hbar W_t}}{m^* a^2 \sqrt{2kT(W_{opt} - W_t)}} \exp\left(-\frac{W_{opt} - W_t}{kT}\right) \times \exp\left(-\frac{2s\sqrt{2m^* W_t}}{\hbar}\right) \sinh\left(\frac{eFa}{2kT}\right). \quad (8)$$

The experimental *lg(j)-F* characteristics of the n-Si/Al_2O_3/Mg structure and the curves simulated by means of the N-G model are presented in Fig. 3(b). The *lg(j) -F* characteristics at various temperatures are described by the N-G model with the following parameters: thermal trap energy of $W_t = 1.5$ eV, optical trap energy of $W_{opt} = 3.0$ eV, trap concentration of $N = 0.7 \times 10^{19}$ cm^{-3}, and effective mass of $m^* = 0.17 m_e$. Consequently, the charge transport mechanism in the n-Si/Al_2O_3/Mg structure synthesized at 250 °C is described by the N-G model of phonon-assisted tunneling between neighboring traps.

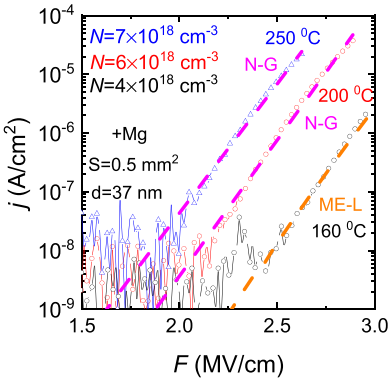

FIG. 4. Current density dependence on the electric field in a-Al_2O_3 films at different synthesis temperatures and the theoretical dependences obtained based on the Makram-Ebeid and Lannoo (ME-L) model of multiphonon isolated trap ionization and the Nasyrov–Gritsenko (N-G) model of phonon-assisted tunneling between neighboring traps. The thermal trap energy is $W_t = 1.5$ eV and the optical trap energy is $W_{opt} = 3.0$ eV for both models.

Similar simulations and their analysis were used for the n-Si/Al_2O_3/Mg structure synthesized at 160 and 200 °C. All fitting parameters are presented in Table I. An increase in the synthesis temperature of a-Al_2O_3 from 160 to 250 °C is accompanied by a transition from the multiphonon isolated trap ionization model to the phonon-assisted tunneling of electrons between neighboring traps model (Fig. 4). In this transition, the thermal $W_t = 1.5$ eV and optical $W_{opt} = 3.0$ eV trap energies do not change. At a low synthesis temperature (160 °C), the trap concentration is relatively low; the trap ionization occurs in the conduction band [Fig. 3(a)]. Increasing the synthesis temperature leads to an increase in the trap concentration [Fig. 3(b)]. In this case, when traps are ionized, it becomes more favorable for the electron tunnel to a neighboring trap, but not into the conduction band [Fig. 3(b)].

It was shown that oxygen vacancies act as traps in a-Al_2O_3.[34] Si–Si bonds act as traps in SiN_x and SiO_x.[35,36] The exponential increase in the current of SiN_x and SiO_x, with the enrichment in silicon, is explained by an increase in the concentration of Si-Si bonds, a decrease in the barrier to the tunneling between traps in the N-G model.

In this paper, the charge transport mechanisms in amorphous a-Al_2O_3 films synthesized at different temperatures were studied. At the synthesis temperature of 160 °C, the charge transport mechanism is described by the Makram-Ebeid and Lannoo model of multiphonon isolated trap ionization. Increasing the synthesis temperature to 200 and 250 °C leads to an increase in the trap concentration, and the Nasyrov–Gritsenko model of phonon-assisted tunneling between neighboring traps is used for describing the charge transport mechanism in a-Al_2O_3 films.

The part of the work related to the charge transport study was carried out under the Russian state contract with the ISP SB RAS

Program No. FWGW-2021-0003. The technological part of the work was carried out under the Russian state contract with ETU LETI No. FSEE-2020-0013. The authors acknowledge core facilities of "VTAN" NSU for the access to its experimental equipment.

AUTHOR DECLARATIONS

Conflict of Interest

The authors have no conflicts to disclose.

Author Contributions

Andrei Gismatulin: Formal analysis (equal); Investigation (equal); Validation (equal); Visualization (equal); Writing – original draft (equal); Writing – review & editing (equal). **Yura Nikolaevich Novikov:** Data curation (equal); Formal analysis (equal); Validation (equal); Writing – review & editing (equal). **Natalia V. Andreeva:** Funding acquisition (equal); Investigation (equal); Methodology (equal); Resources (equal); Supervision (equal); Validation (equal); Writing – original draft (equal); Writing – review & editing (equal). **Dmitriy Mazing:** Investigation (equal); Methodology (equal); Resources (equal); Visualization (equal); Writing – review & editing (equal). **V. A. Gritsenko:** Conceptualization (equal); Funding acquisition (equal); Project administration (equal); Supervision (equal); Validation (equal); Writing – original draft (equal); Writing – review & editing (equal).

DATA AVAILABILITY

The data that support the findings of this study are available from the corresponding author upon reasonable request.

REFERENCES

[1]V. A. Gritsenko, "Silicon nitride on Si: Electronic structure for flash memory devices," in *Thin Films on Si: Electronic and Photonic Applications* (World Scientific Press, 2016), pp. 273–322.
[2]A. Goda, "Recent progress on 3D NAND flash technologies," Electronics **10**, 3156 (2021).
[3]S. Kim and B.-G. Park, Appl. Phys. Lett. **108**, 212103 (2016).
[4]M. Y. Yang, K. Kamiya, B. Magyari-Koepe *et al.*, Jpn. J. Appl. Phys., Part 1 **52**(4S), 04CD11 (2013).
[5]J. Molina-Reyes and L. Hernandez-Martinez, Complexity **2017**, 263904.
[6]Y. Wu, B. Lee, and H.-S. P. Wong, IEEE Electron Device Lett. **31**(12), 1449–1451 (2010).
[7]J. Park, D. Huh, S. Son, W. Kim, S. Ju, and H. Lee, Global Challenges **6**(7), 2100118 (2022).
[8]A. S. Sokolov, S. K. Son, D. Lim *et al.*, J. Am. Ceram. Soc. **100**, 5638–5648 (2017).
[9]Y. Wu, S. M. Yu, H. S. P. Wong, Y. S. Chen, H. Y. Lee, S. M. Wang, P. Y. Gu, F. Chen, and M. J. Tsai, in IEEE International Memory Workshop (2012).
[10]Y. Lee, J. Park, D. Chung *et al.*, Nanoscale Res. Lett. **17**, 84 (2022).
[11]B. J. Choi, A. C. Torrezan, J. P. Strachan, P. G. Kotula, A. J. Lohn, M. J. Marinella *et al.*, Adv. Funct. Mater. **26**(29), 5290–5296 (2016).
[12]J. Borghetti, G. S. Snider, P. J. Kuekes, J. J. Yang, D. R. Stewart, and R. S. Williams, Nature **464**(8), 863 (2010).
[13]A. Rodriguez, M. B. Gonzalez, E. Miranda, F. Campabadal, and J. Suce, Microelectron. Eng. **147**, 75–78 (2015).
[14]J. Yao, Z. S. L. Zhong, D. Natelson, and J. M. Tour, Nano Lett. **10**, 4105–4110 (2010).
[15]N. V. Andreeva, A. A. Romanov, D. S. Mazing *et al.*, Nanotechnol. Rep. **16**(6), 790–797 (2021).
[16]B. A. Sperling, B. Kalanyan, and J. E. Maslar, J. Phys. Chem. C **124**(5), 3410–3420 (2020).
[17]M. D. Groner, F. H. Fabreguette, J. W. Elam, and S. M. George, Chem. Mater. **16**, 639–645 (2004).
[18]Y. N. Novikov, V. A. Gritsenko, and K. A. Nasyrov, Appl. Phys. Lett. **94**, 222904 (2009).
[19]Y. Novikov, A. A. Gismatulin, V. A. Gritsenko, B. Hallac, and Y. Roizin, Thin Solid Films **781**, 140004 (2023).
[20]K. Kukli, M. Ritala, and M. Leskela, J. Vac. Sci. Technol. A **15**(4), 2214 (1997).
[21]G. A. Brown, W. P. Robinette, and G. Carlson, J. Electrochem. Soc. **115**, 948 (1968).
[22]D. J. DiMaria, D. W. Dong, C. Falcony, T. N. Theis, J. R. Kirtley, J. C. Tsang, D. R. Young, F. L. Pesavento, and S. D. Brorson, J. Appl. Phys. **54**, 5801 (1983).
[23]K. L. Jensen, J. Appl. Phys. **102**, 24911 (2007).
[24]T. V. Perevalov and V. A. Gritsenko, Phys.-Usp. **53**, 561 (2010).
[25]G. G. Roberts and J. I. Polango, Phys. Stat. Sol. A **1**, 409–420 (1970).
[26]V. A. Gritsenko, E. E. Meerson, and Y. N. Morokov, Phys. Rev. B **57**(4), R2081–R2083 (1998).
[27]T. V. Perevalov, A. A. Gismatulin, D. S. Seregin, Y. Wang, H. Xu, V. N. Kruchinin, E. V. Spesivcev, V. A. Gritsenko, K. A. Nasyrov, I. P. Prosvirin, J. Zhang, K. A. Vorotilov, and M. R. Baklanov, J. Appl. Phys. **127**, 19 (2020).
[28]J. Frenkel, Phys. Rev. **54**, 647 (1938).
[29]J. Frenkel, Tech. Phys. USSR **5**(8), 685–695 (1938).
[30]R. M. Hill, Philos. Mag. **23**(181), 59–86 (1971).
[31]H. Adachi, Y. Shibata, and S. Ono, J. Phys. D **4**(7), 988–994 (1971).
[32]S. S. Makram-Ebeid and M. Lannoo, Phys. Rev. B **25**, 6406 (1982).
[33]K. A. Nasyrov and V. A. Gritsenko, J. Appl. Phys. **109**(9), 093705 (2011).
[34]T. V. Perevalov, O. E. Tereshenko, V. A. Gritsenko, V. A. Pustovarov, A. P. Yelisseyev, C. Park, J. H. Han, and C. Lee, J. Appl. Phys. **108**, 013501 (2010).
[35]V. A. Gritsenko, N. V. Perevalov, O. M. Orlov, and G. Krasnikov, Appl. Phys. Lett. **109**, 06294 (2016).
[36]V. A. Gritsenko, V. A. Nadolinny, K. S. Zhuravlev, J. B. Xu, and H. Wong, J. Appl. Phys. **109**, 084502 (2011).